Theor Chim Acta (1993) 85: 69–86

Theoretica Chimica Acta

© Springer-Verlag 1993

Theoretical studies of [*n*]paracyclophanes and their valence isomers

II. Study of the reactions of benzene, [6]- and [7]paracyclophanes to their Dewar benzene and prismane isomers in the ground state*

F. Bockisch[1,2], J.-C. Rayez[1], H. Dreeskamp[2], D. Liotard[1], and B. Duguay[1]

[1] Laboratoire de Physicochimie Théorique, Université Bordeaux I, 351, cours de la Libération, F-33405 Talence Cédex, France

[2] Institut für Physikalische und Theoretische Chemie, Technische Universität Braunschweig, Hans Sommer Str. 10, W-3300 Braunschweig, Germany

Received July 26, 1991/Accepted May 19, 1992

Summary. The valence isomerisations of benzene, [6]- and [7]paracyclophane to their Dewar benzene and prismane isomers are studied with the MNDO method using the unrestricted Hartree–Fock (UHF) and the configuration interaction (C.I.) approximations. The enthalpy of the reaction Dewar benzene → benzene is $\Delta H_r^\circ = -68.9$ kcal/mol and the activation enthalpy is $\Delta H^{\circ\ddagger} = 27.9$ kcal/mol (with C.I.). The reaction path has C_{2v} symmetry.

The determination of several points of the lowest potential energy surface of [6]- and [7]paracyclophanes leads to a minimum reaction path having the same topology as for the potential energy surface of the nonbridged benzene. The only difference is a quantitative change in the energy values of the aromatic isomers due to the deformation introduced by the alkyl chain. For [6]paracyclophane, the activation enthalpy is $\Delta H^{\circ\ddagger} = 24.6$ kcal/mol and the activation entropy is $\Delta S^{0\ddagger} = 0.6$ cal K^{-1} mol^{-1} calculated with C.I.

The enthalpy of the reaction prismane → Dewar benzene is $\Delta H_r^\circ \approx -32$ kcal/mol and the activation enthalpy is $\Delta H^{\circ\ddagger} \approx 19$ kcal/mol. The highest molecular symmetry group common to both molecules is C_{2v}, whereas the symmetry group of the reaction path is lowered to C_s. Along this reaction path is located a biradicaloid intermediate, separated by low activation barriers from the products. No significant changes of the potential energy surfaces are found for the bridged [*n*]prismanes and the [*n*]Dewar benzenes.

All the calculated values, reaction enthalpies, activation enthalpies and entropies, are in a good agreement with literature experimental data.

Key words: [*n*]Paracyclophanes – Dewar benzene isomers – Prismane isomers – Semiempirical methods – Transition states – Biradicaloid intermediates

1 Introduction

Many aromatic compounds can be directly transformed into their Dewar benzene isomers by irradiation. For example, benzene gives Dewar benzene. This reaction has been experimentally studied in detail for many substituted benzenes [1–5]. A

* This article is dedicated to Professor A. Pullman

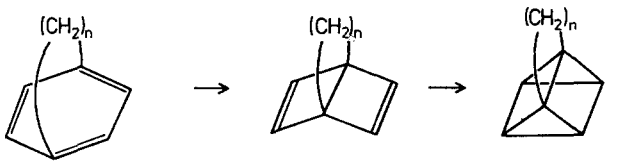

Fig. 1. Formula of the relevant compounds

summary of the isomerisation of benzene to its Dewar benzene isomer as well as other isomerisation reactions is given in [6]. Higher aromatic hydrocarbons such as naphthalene can also be isomerised into their Dewar benzene forms [7].

The yields of these reactions increase if deformed aromatic compounds undergo the valence isomerisation. Jahn et al. found that 9-*t*-butyl-anthracene, with a deformation angle of 13°, can easily give its Dewar isomer [8]. Another possibility of introducing a deformation is the bridging of the meta- or para-positions of a benzene ring by a short alkyl chain. The latter, the so-called [*n*]paracyclophanes, $(CH_2)_n C_6H_4$, are treated in this paper (Fig. 1). For example, [6]paracyclophanes have a deformation angle of the aromatic system of about 20° [9, 10]. From [6]paracyclophane derivatives, the Dewar benzene isomers can be obtained photochemically (Fig. 1). These [*n*]Dewar benzenes are fairly stable at room temperature but can rearomatise into the [6]paracyclophane derivatives at higher temperatures. This reaction is well known and experimentally the thermodynamical as well as the kinetic parameters for disubstituted compounds have been determined in previous studies [11, 12].

From those Dewar benzenes, another (photochemical) valence isomerisation is possible: the formation of prismane (Fig. 1). In recent work, it has been shown that also para-bridged Dewar benzenes, the so-called [*n*]Dewar benzenes, give this valence isomerisation [9–12].

Also many theoretical studies have been done on the unbridged compounds (see for example for benzene, Dewar benzene and their interconversion [13–18]) and numerical data as the activation enthalpy (from SCF calculations with configuration interaction) have been estimated [18]. Calculations of the geometries of prismane derivatives have been performed by Bews et al. [19] and in other work (see [17]).

In the case of the para-bridged compounds, no analysis of the analogous reaction paths has yet been done. Only the [*n*]paracyclophanes themselves have been treated with theoretical approaches. In 1973, Allinger et al. used simple molecular mechanics models to optimize the geometries of [*n*]paracyclophanes [20]. Later, also the strain energies [21] and electronic excitations towards excited states have been calculated [21]. Semiempirical methods have been mainly applied by Bickelhaupt [22] and Schmidt [23] in order to obtain the geometries, deformation angles, strain energies and photo electron spectra. Schaefer III et al. used *ab initio* methods with minimum and double zeta basis sets in the calculations of the geometries and the strain energies [24].

Because of this lack of information on the reaction path and in particular on the transition state of the reactions of [*n*]paracyclophanes, we use semiempirical methods for the determination of molecular energies, which allow us to give reliable estimates of the enthalpies ΔH_r° and entropies ΔS_r° of the reaction Dewar benzene → benzene and their activation counterparts $\Delta H^{\circ\ddagger}$ and $\Delta S^{\circ\ddagger}$. Moreover, changes of molecular geometries along the reaction path are analyzed. The

theoretical results obtained for this reaction of the unstrained benzene are then compared to the calculated values of the strained [7]paracyclophane (deformation angle $\alpha \approx 15°$ [25]) and [6]paracyclophane ($\alpha \approx 23°$ [9, 10]). A detailed comparison with experimental data is also given in order to verify the reliability of our results.

In the case of the reaction of Dewar benzene, [6]- and [7]Dewar benzene to their prismane isomers, the calculation methods for the localization of transition states allow us to determine their geometry and to propose the existence of a reaction intermediate. The numerical values obtained from our theoretical calculations are compared to experimental data in order to establish the reliability of our results. The influence of the introduction of an alkyl bridge is also discussed.

2 Theoretical background

2.1 Computational methods

All the theoretical results presented in this paper are obtained using the semiempirical method MNDO [26, 27]. In a preliminary comparative study, we showed than any of the semiempirical methods tested (AM1, PM3, MNDO and MINDO/3) can be used for the determination of the geometries in [n]paracyclophanes [28]. In the application to the calculation of the enthalpies, MNDO gives the results in best agreement with experimental data. Therefore, we decided to use only the MNDO method throughout in this paper.

Although the restricted Hartree–Fock approximation (RHF) can lead to reliable results for closed shell systems, this approach can no longer be used in the study of reaction paths where biradicaloid structures could have to be involved. Therefore we also used the unrestricted Hartree–Fock approach (UHF) [29] and a limited configuration interaction (C.I.) based upon RHF calculations [30].

2.2 Localization methods of the transition states

An unambiguous definition of a reaction path requires a dynamical point of view as proposed by McIver [31], Morokuma [32], Fukui [33–35] and Basilevsky [36]. It is identified as the vanishing kinetic energy trajectory which links two energy minima via a saddle point. Such an "'intrinsic reaction coordinate" (IRC) (which could be renamed more properly as "intrinsic reaction path") corresponds to the two steepest-descent paths that emerge from a saddle point in both directions along the principal axis of negative curvature as a tangent. This property holds only in terms of mass-weighted Cartesian coordinates [37]. However, in this work, we try not find any IRC, but we focus on the saddle point's structures. Since a saddle point corresponds to a stationary point, it is coordinate-independent.

In the search for a saddle point, one can first select a geometrical parameter as the reaction coordinate and, for a fixed value of this parameter, optimize all the other geometrical coordinates. This method can fail to locate a saddle point (because of a discontinuous path [38]). Therefore, we use a more sophisticated method, called the "chain method", implemented by one of us in AMPAC 2.1 [27]. Its strategy is the following: reactant and product both correspond to

minima of the potential energy surface. A path connecting them in the configuration space of all geometrical coordinates is provided by the linear interpolation from the reactant to an initially estimated trial point for the saddle point, and similarly to the product. The highest point in energy along the path can be displaced in the direction of the steepest-descent transverse to the path and so an improved path – not a point – is obtained. The process is pursued until no more transverse energy relaxation is observed. This highest point of the asymptotic path corresponds to a saddle point linking reactant and product; it is also the highest saddle point to be crossed through, if several do exist, along the reaction path.

For the saddle points found by this method, we checked in every case that they have only one negative eigenvalue of the Hessian matrix [39].

2.3 Thermodynamic calculations

All thermodynamic quantities are obtained from the calculation of energy referenced to 300 K. The entropies are estimated by the calculation of their contributions of translation, rotation and vibration of the molecules:

$$S_{tot} = S_{trans} + S_{rot} + S_{vib} \tag{1}$$

The contributions of the rotational motions require knowledge of the moments of inertia, i.e. the geometries, of the stationary points and the contribution of the vibrational motion is evaluated from the force field associated with these structures [40].

3 Results and discussion

3.1 The valence isomerisation benzene → Dewar benzene

The chain method coupled with the UHF- or C.I.-technique provides the energy of some points of the path connecting benzene and Dewar benzene. These points, which are not too far from the intrinsic reaction path, are used to analyze the evolution of the energies of the RHF molecular orbitals (MOs) with the distance between the *para* carbon atoms. Figure 2a depicts this evolution. The symmetry point group C_{2v}, with a C_2 axis which is coaxial with the C_6 axis of benzene, is found to be conserved through the path. A crossing of molecular orbitals of symmetries a_1 and b_1 close to the Fermi level occurs at $r_7 = 2.1$ Å (Fig. 3), indicating that such an isomerisation is a forbidden process according to the Woodward–Hoffmann rules [41].

The full active space (F.A.S.) configuration interaction, which we performed, is developed on the two highest occupied and the two lowest virtual orbitals. A greater active space based on the three highest occupied and the three lowest unoccupied MOs does not change significantly the results. Therefore, all calculations with configuration interaction are done with these four orbitals.

The geometries of the transition state, benzene and Dewar benzene are given in Table 1. Both UHF and C.I. methods give consistent results with differences in the bond angles less than 1° and in the bond lengths less than 0.03 Å. The reaction path can be correctly represented mainly by the variations of two internal coordinates: the interatomic distance r_7 and the dihedral angle

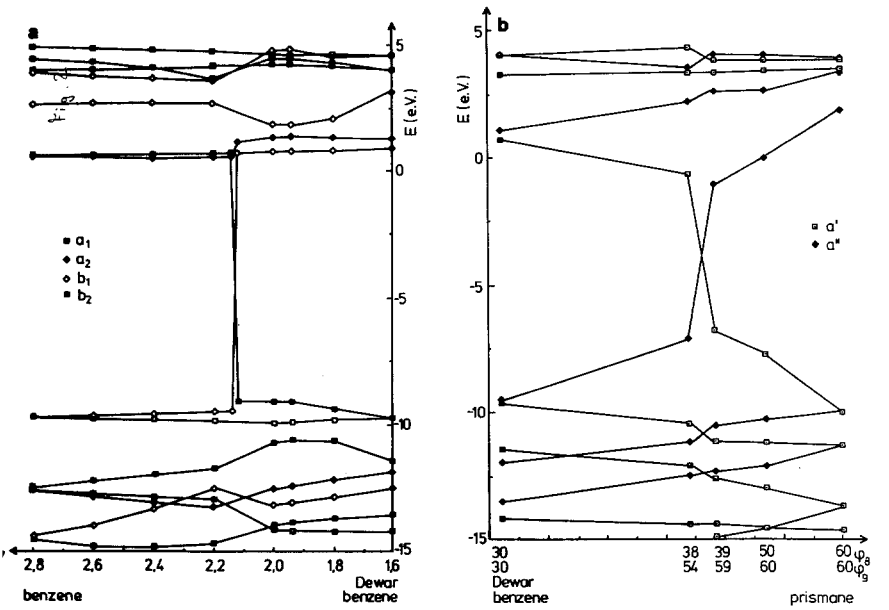

Fig. 2. Correlation diagram for the reactions: (*a*) benzene → Dewar benzene and (*b*) Dewar benzene → prismane

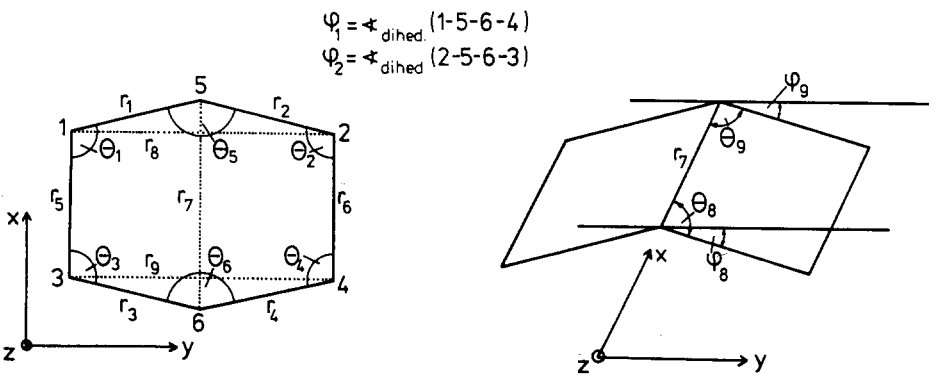

Fig. 3. Definition of the geometrical parameters

φ ($=\varphi_8 = \varphi_9$ in Fig. 3) as shown below. Figure 4 gives the r_7, φ-contour map of isoenergy with a C_{2v} symmetry constraint, all the other coordinates being fully optimized. In this figure, we drew the steepest-descent path (*dashed line*) which is tangent to the "transition vector" at the transition state. Strictly speaking, the transition vector is the normal mode at the transition state with an imaginary frequency. Nevertheless, we kept in this text the name "transition vector" although it would have been more appropriate to speak about "principal axis of least curvature". This transition vector is almost represented by the variation of r_7. In the regions of benzene and Dewar benzene, the evaluation of the reaction path is almost only the one of φ (the lowest normal mode with a_1 symmetry).

Table 1. Geometries of the C_6 cycles in benzene, [7]- and [6]paracyclophane, its Dewar benzene isomers and the transition states connecting them (α, β and γ are the deformation angles of the aromatic system, the alkyl chain and the whole molecule [28]); lengths in Å, angles in degrees; see definitions in Fig. 3)

	RHF	UHF	C.I.	exp.
benzene (D_{6h})				
r_1	1.41	1.41	1.41	1.40[a]
r_7	2.81	2.83	2.82	2.80[a]
θ_1	120.0	120.0	120.0	120.0[a]
φ_1	180.0	180.0	180.0	180.0[a]
α	0.0	0.0	0.0	0.0[a]
transition state (C_{2v})				
r_1	—	1.49	1.30	—
r_5	—	1.38	1.35	—
r_7	—	1.94	1.97	—
θ_1	—	100.9	101.9	—
θ_5	—	119.7	119.7	—
φ_1	—	123.4	124.1	—
α	—	67.9	65.9	
Dewar benzene (C_{2v})				
r_1	1.53	1.52	1.52	1.52[b]
r_5	1.36	1.37	1.38	1.35[b]
r_7	1.61	1.61	1.61	1.63[b]
r_8	2.61	2.60	2.61	—
θ_1	94.7	94.5	94.4	—
θ_5	117.2	117.3	117.9	—
φ_1	117.9	117.8	118.4	117.7[c]
φ_8	31.1	31.1	30.8	—
α	81.0	81.4	81.6	—
[7]paracyclophane (C_s)				
r_1	1.42	1.43	1.42	1.42[d]
r_2	1.42	1.43	1.42	1.42[d]
r_5	1.40	1.41	1.40	1.40[d]
r_7	2.79	2.81	2.80	2.84[d]
θ_1	119.3	119.1	119.3	119[d]
θ_2	119.3	119.1	119.3	120[d]
θ_5	117.3	116.8	117.3	118[d]
φ_1	156.9	154.5	156.6	—
α	19.6	21.6	19.8	—
β	10.7	9.9	10.7	—
γ	30.4	31.4	30.6	—
[7]transition state (C_s)				
r_1	—	1.50	1.50	—
r_2	—	1.51	1.51	—
r_5	—	1.37	1.35	—
r_7	—	1.93	2.01	—
θ_1	—	100.7	102.6	—
θ_2	—	100.6	102.6	—
θ_5	—	114.2	115.1	—
φ_1	—	117.6	119.7	—
α	—	70.1	66.0	—
β	—	19.5	12.9	—
γ	—	51.1	53.7	—
[7]Dewar benzene (C_s)				
r_1	1.53	1.53	1.54	—
r_2	1.54	1.54	1.54	—
r_5	1.35	1-35	1.38	—
r_7	1.64	1.64	1.61	—
θ_1	95.3	95.3	94.2	—
θ_2	95.3	95.3	94.3	—
θ_5	112.5	112.5	111.9	—
φ_1	113.2	113.2	112.4	—
α	80.4	80.4	82.4	—
β	29.2	29.2	30.9	—
γ	51.5	51.5	51.7	—
[6]paracyclophane (C_2)				
r_1	1.42	1.44	1.43	1.40[e]
r_2	1.42	1.44	1.43	1.40[e]
r_5	1.40	1.41	1.40	1.38[e]
r_7	2.74	2.75	2.74	—
θ_1	118.0	117.7	118.0	119.9[e]
θ_2	118.1	117.8	118.1	119.9[e]
θ_5	113.1	113.1	112.5	116.6[e]
φ_1	150.4	147.0	150.0	—
α	25.6	28.4	25.9	20.9[e]
β	16.0	14.7	16.0	18.1[e]
γ	41.6	43.1	41.9	—
[6]transition state (C_2)				
r_1	—	1.50	1.49	—
r_2	—	1.50	1.50	—
r_5	—	1.37	1.36	—
r_7	—	1.93	2.10	—
θ_1	—	100.7	104.2	—
θ_2	—	100.7	104.4	—
θ_5	—	115.4	115.0	—
φ_1	—	118.7	121.0	—

Table 1 (continued)

	RHF	UHF	C.I.	exp.
[6]transition state (C_2)				
α	—	69.7	62.7	—
β	—	19.8	12.6	—
γ	—	49.9	50.2	—
[6]Dewar benzene (C_2)				
r_1	1.53	1.53	1.53	—
r_2	1.53	1.53	1.54	—
r_5	1.36	1.37	1.38	—
r_7	1.63	1.64	1.61	—
θ_1	95.1	95.0	94.2	—
θ_2	95.1	95.0	94.3	—
θ_5	117.1	116.2	116.9	—
φ_1	113.9	113.8	113.0	—
α	80.7	80.9	82.3	—
β	30.6	30.8	32.1	—
γ	50.1	50.1	50.3	—

[a] ref. [54]
[b] ref. [55]
[c] ref. [60]
[d] ref. [25] for 8-carboxy[6]paracyclophane
[e] ref. [56] for 3-carboxy[7]paracyclophane

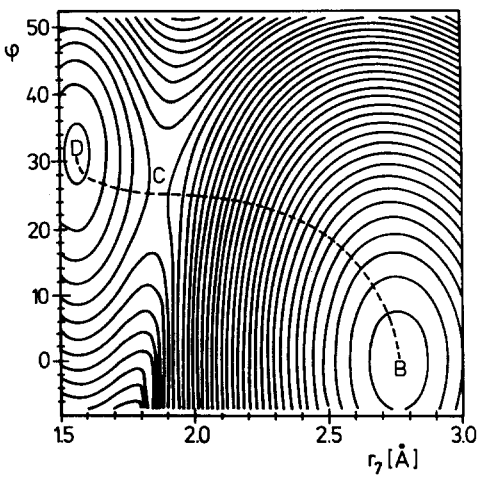

Fig. 4. Energy contour diagram for the reaction benzene → Dewar benzene calculated with the UHF approach (from 19.5 to 103.5 kcal/mol) in steps of 3.0 kcal/mol) (D = Dewar benzene, C = transition state, B = benzene; --- = steepest-descent path using this choice of coordinates)

It is clear from this study that neither r_7 nor φ can be retained alone as "reaction coordinate" (compared to [42]).

The transition state is much closer to Dewar benzene than to benzene, in agreement with Hammond's rule [43, 44].

The reaction path belongs to the C_{2v} symmetry, the maximum allowed group according to symmetry rules [45]. However, the chain method is a local search algorithm, and another path may still exist, with a lower symmetry, thus avoiding the crossing of MOs and lowering the activation barrier. In order to check this hypothesis, we proceed as follows: the MOs, which cross along the reaction path, belong to the symmetry species a_1 and b_1 (in the C_{2v}, group). The reduction of the symmetry C_{2v} may lead to any of its subgroups (C_2, C_s keeping the σ_{xz} plane and C_s' keeping the σ_{yz} plane). However, the crossing is only avoided in C_s where the symmetry species become of the same irreductible representation a'. In spite of great efforts, no transition state has been found in this symmetry C_s. We can therefore conclude that, although the absence of a

Table 2. Geometries of the C_6 skeletons of the stationary points of the potential energy surface of the reaction prismane → Dewar benzene (lengths in Å, angles in degrees)

	RHF	UHF	C.I.	exp.
Dewar benzene $D(C_{2v})$				
see Table 1				
prismane P (C_{2v})				
r_1	1.55	1.55	1.55	1.54[a]
r_5	1.55	1.55	1.55	1.55[a]
r_7	1.55	1.55	1.55	1.55[a]
r_8	1.55	1.55	1.55	1.54[a]
θ_1	90.0	90.0	90.0	90.0[a]
θ_5	60.0	60.0	60.0	60.0[a]
φ_8	60.0	60.0	60.0	60.0[a]
transition state C1 (D→I) (C_s)				
r_1	—	1.53	1.53	—
r_3	—	1.52	1.53	—
r_5	—	1.46	1.47	—
r_7	—	1.60	1.58	—
r_8	—	2.41	2.41	—
r_9	—	1.82	1.74	—
θ_1	—	91.2	90.4	—
θ_3	—	91.9	90.9	—
θ_5	—	104.3	103.8	—
θ_6	—	73.5	69.5	—
φ_8	—	37.7	38.0	—
φ_9	—	53.1	55.2	—
hilltop H (C_{2v})				
r_1	—	1.52	1.52	—
r_5	—	1.49	1.49	—
r_7	—	1.59	1.57	—
r_8	—	1.86	2.94	—
θ_1	—	91.9	91.6	—
hilltop H (C_{2v})				
θ_5	—	75.4	79.2	—
φ_8	—	52.3	50.4	—
intermediate I (C_s)				
r_1	—	1.52	1.52	—
r_3	—	1.54	1.55	—
r_5	—	1.49	1.49	—
r_7	—	1.60	1.60	—
r_8	—	2.36	2.37	—
r_9	—	1.59	1.57	—
θ_1	—	90.6	90.7	—
θ_3	—	89.5	88.9	—
θ_5	—	101.6	102.5	—
θ_6	—	62.1	60.8	—
φ_8	—	39.1	38.6	—
φ_9	—	58.9	59.5	—
transition state C2 (I→P) (C_s)				
r_1	—	1.52	1.55	—
r_3	—	1.55	1.55	—
r_5	—	1.52	1.55	—
r_7	—	1.58	1.55	—
r_8	—	1.92	1.55	—
r_9	—	1.56	1.55	—
θ_1	—	91.4	91.2	—
θ_3	—	89.9	89.4	—
θ_5	—	78.3	85.8	—
θ_6	—	60.5	59.3	—
φ_8	—	50.8	47.1	—
φ_9	—	59.7	60.4	—

[a] ref. [47] for hexamethylprismane

transition state can never be proven [45], it would be unlikely to find on the potential energy surface another transition state with C_s symmetry. The only transition state found in the reaction benzene → Dewar benzene keeps the maximum symmetry C_{2v} associated with the relevant MOs crossing.

3.2 The valence isomerisation prismane → Dewar benzene

The calculated geometrical parameters of Dewar benzene and prismane are given in Table 2. These results show that the RHF-, UHF- and the RHF-C.I. approaches give consistent values. They are in very good agreement with

experimental data known for Dewar benzene [46] and prismane [47]. The errors in the bond lengths are less than 0.03 Å and the errors in the angles are less than 0.7°.

The full active space (F.A.S.) configuration interaction is developed on the two highest occupied and the two lowest unoccupied MOs. This keeps consistency with the treatment of the preceding isomerisations and accounts with the HOMO-LUMO crossing which could be encountered along the isomerisation path (Fig. 1b).

The highest symmetry for a path from Dewar benzene (D) to prismane (P) has the symmetry C_{2v}. Under these symmetry constraints, the "chain" method locates a stationary point H which directly links Dewar benzene and prismane without passing through another minimum. However, in the full 30-dimensional configuration space, the Hessian matrix has two negative eigenvalues at the point H and, therefore, H is not a transition state for this isomerisation process. Using the set of internal coordinates pictured in Fig. 3, the eigenvectors corresponding to the two negative eigenvalues of the Hessian matrix at the point H are mainly described as:

$$\begin{aligned} v_1 &\approx 0.64 \cdot (\varphi_8 + \varphi_9) \\ v_2 &\approx 0.70 \cdot (\varphi_8 - \varphi_9) \end{aligned} \tag{2}$$

the remaining coefficients being negligible. Since the Hessian matrix is real and symmetric, the eigenvectors are mutually orthogonal. Therefore, the coefficients displayed in the above expressions give the magnitude of the gap between the v_1 and v_2 vectors and the vectors $(1/\sqrt{2})(\varphi_8 \pm \varphi_9)$ respectively. The first vector, v_1, looks like a transition vector for the reaction Dewar benzene → prismane. However, the second vector, v_2, points in a direction where the symmetry of the molecule is downgraded to C_s, conserving the symmetry plane σ_{xz} (Fig. 3).

Restarting the chain method without any symmetry constraint, such a true transition state $C1$ is found, with C_s symmetry as expected, and with the transition vector:

$$v_{C1} \approx -0.01\varphi_8 - 0.97\varphi_9 \tag{3}$$

By reasons of symmetry, an equivalent transition state $C1'$ does exist on the potential energy surface with $\varphi_8(C1') = \varphi_9(C1)$ and $\varphi_9(C1') = \varphi_8(C1)$. Starting from $C1$ in the direction of v_{C1} and integrating the steepest-descent path in the internal coordinates of Fig. 3 ("PATH" method in AMPAC [27]), the prismane (P) is reached. However, starting in the opposite direction, $-v_{C1}$, and following the steepest-descent path, a stable intermediate I is reached instead of the minimum D. The geometry of I is quoted in Table 1. One C–C σ bond has nearly reached its value at P while the other C–C bond is almost the same as in D: a typical biradicaloid situation.

Therefore, the mechanism of the reaction Dewar benzene → prismane is analogous to the classical dimerisation of ethylene to cyclobutene where the existence of a biradicaloid intermediate has also been postulated from *ab initio* calculations [48]. The lowest state of I is a triplet ($\Delta H_f^\circ = 133.9$ kcal/mol, see further Table 4). The singlet state is 2.3 kcal/mol higher in energy and has almost the same geometry (see further Table 4).

The Morse theory [49] and the common sense indicate that at least one more transition state, $C2$, lies between the intermediate I and Dewar benzene D. It is easily found by the chain method (working between D and I, not P), with C_s

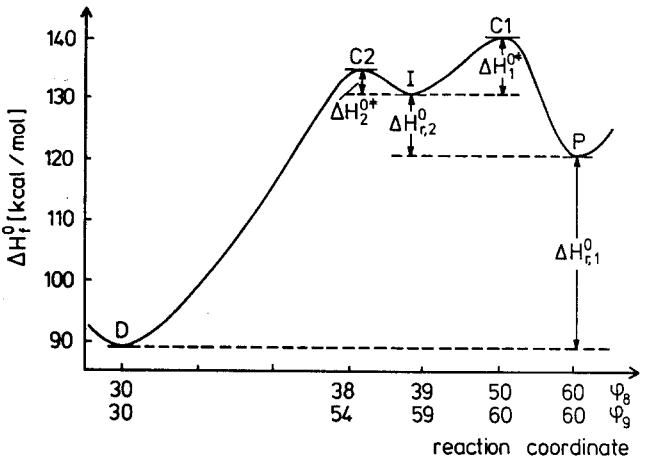

Fig. 5. Scheme representing the definition of the heats of reaction and the activation enthalpies used in the discussion

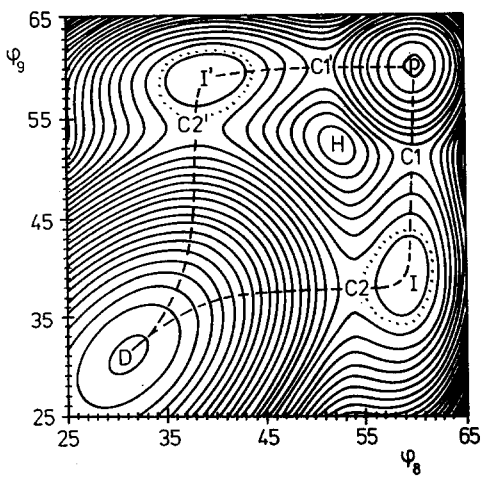

Fig. 6. Energy contour diagram for the reaction prismane → Dewar benzene calculated with the UHF approach (from 89.5 to 152.0 kcal/mol in steps of 2.5 kcal/mol) (D = Dewar benzene, P = prismane, I = intermediate, H = hilltop, C1, C2 = transition states, – – – = steepest-descent path, · · · = singlet-triplet intersection line)

symmetry and with the "transition vector" Fig. 3:

$$v_{C2} \approx 0.83\varphi_8 + 0.08\varphi_9 \tag{4}$$

No other stationary points were found along the steepest-descent paths starting from C_2.

The energy profile for this two-step mechanism is shown in Fig. 5. The dihedral angles φ_8 and φ_9 play the major role in describing the "unstable" eigenvectors of the Hessian matrix at the points H, $C1$ and $C2$ and the symmetrically related points $C1'$ and $C2'$. Similarly to Fig. 4, a two-dimensional map of the potential energy surface can be constructed with φ_8 and φ_9, which subsumes the entire reaction paths network. Such a map includes the points D, I, I′ and P and reflects the correct topology of the mechanism of the reaction Dewar benzene → prismane in the number of stationary points and indices (the number of negative eigenvalues of the Hessian matrix) and in the connectivity between these points (using the steepest-descent paths) (Fig. 6).

3.3 *The valence isomerisations [n]paracyclophane → [n]Dewar benzene → [n]prismane (n = 6, 7)*

The results of the calculations for the bridged compounds show that the Dewar benzene skeletons in the [n]Dewar benzenes can be regarded as undeformed by the alkyl chain (Table 1). However, the aromatic C_6 rings in the [n]paracyclophanes show a strong deformation from planarity. The maximum symmetry of these rings (without considering the alkyl chain), C_{2v}, is almost kept after deformation and the symmetry of the entire molecule (the alkyl chain included) is C_2 (for $n = 6$; with the C_2 axis of C_{2v}) or C_s (for $n = 7$; with the σ_{xz} plane of C_{2v}). However, we do not impose any symmetry in the calculations leaving the systems to relax.

It turns out that these total symmetries hold along the reaction path. Moreover, the symmetry C_{2v} is still found for the skeletons of the transition states of the reactions [n]paracyclophane → [n]Dewar benzene ($n = 6, 7$). Consequently, the MO correlation diagrams are qualitatively the same in the reaction of the [n]paracyclophanes (with $n = 6$ and 7) as for benzene.

The equilibrium geometries of the unbridged Dewar benzene and prismane are given in Table 2. Although a great deformation of the aromatic system is obtained in the (bridged) [n]paracyclophanes, the Dewar benzene- and the prismane-skeletons in the bridged compounds (in analogy to the study of the reactions [n]paracyclophane → [n]Dewar benzene for $n = 6$ and 7) can be regarded as undeformed by the alkyl chain.

3.4 *Energetic analysis of the reaction path [n]paracyclophane → [n]Dewar benzene*

The enthalpies of the valence isomerisation [n]Dewar benzene → [n]paracyclophane have already been discussed in the first article of this series ($n = 3$ to 10) [28]. They are given together with the activation parameters in Table 3.

The entropies ΔS_r° at 300 K, calculated for these reactions, are also given in Table 3. It is obvious that in the case of the valence isomerisation of benzene, Dewar benzene has a slightly higher absolute entropy S° than benzene, leading to a reaction entropy ΔS_r° of about -3 cal K^{-1} mol^{-1}. The deformation of the benzene ring in the [7]paracyclophane with respect to the unbridged cycle leads to a reaction entropy ΔS_r° of -6 cal K^{-1} mol^{-1}, a small decrease with respect to the value for the reaction Dewar benzene → benzene. In the case of [6]paracyclophane, ΔS_r° is lower (about -2 cal K^{-1} mol^{-1}). This is due to the rotational contributions S_{rot} in the entropies (see Eq. (1)) because the symmetry number σ is 2 in the reactions Dewar benzene → benzene (symmetry C_{2v}) and [6]Dewar benzene → [6]paracyclophane (symmetry C_2), but it is only 1 in the reaction [7]Dewar benzene → [7]paracyclophane (symmetry C_s). Nevertheless, these entropies stay small as expected for isomerisations which are typically in the range of $\Delta S_r^\circ = -5$ to $+3$ cal K^{-1} mol^{-1} [50] (compared to the bimolecular reaction ethylene + ethylene → cyclobutene: $\Delta S_r^\circ = -34.5$ cal K^{-1} mol^{-1} at 623 K [51]).

Besides the heats of formation and the enthalpies of the reactions, Table 3 gives also the enthalpies of activation $\Delta H^{\circ\ddagger}$ of the reaction Dewar benzene → benzene, i.e. $\Delta H^{\circ\ddagger} = \Delta H_f^\circ$ (transition state) − ΔH_f° (Dewar benzene). We observe an acceptable agreement between the experimental change of the heats of the reactions ΔH_r° between the reactions of (unbridged) benzene and [6]paracyclophane ($\Delta H_r^\circ = -60 + 17 = -43$ kcal/mol) and the theoretical

Table 3. Enthalpies (in kcal mol^{-1}) and entropies (in cal K^{-1} mol^{-1} at 300 K) of the valence isomerisation of benzene, [7]- and [6]paracyclophane to its Dewar benzene isomers

	Compound/reaction	RHF	UHF	C.I.	exp.
ΔH_f°	benzene	21.3	19.4	5.9	19.3[a]
	transition state	—	103.5	102.7	—
	Dewar benzene	89.6	89.2	74.8	(79.3)[b]
ΔH_r°	Dewar benzene → benzene	−68.3	−69.8	−68.9	(−60)[c]
	[7]Dewar benzene → [7]p.c.	−52.3	−57.5	−54.1	—
	[6]Dewar benzene → [6]p.c.	−34.9	−43.4	−37.3	(−17)[d]
$\Delta H^{\circ\ddagger}$	Dewar benzene → benzene	—	14.3	27.9	37.8[e]
	[7]Dewar benzene → [7]p.c.	—	9.2	21.4	—
	[6]Dewar benzene → [6]p.c.	—	9.3	21.7	21.1[f]
S°	benzene	60.6	61.2	60.6	—
	transition state	—	64.9	65.9	—
	Dewar benzene	63.8	64.0	63.9	—
ΔS_r°	Dewar benzene → benzene	−3.2	−2.9	−3.2	—
	[7]Dewar benzene → [7]p.c.	−4.7	−6.8	−5.3	—
	[6]Dewar benzene → [6]p.c.	−2.3	−0.2	−2.5	—
$\Delta S^{\circ\ddagger}$	Dewar benzene → benzene	—	0.9	2.0	—
	[7]Dewar benzene → [7]p.c.	—	−2.8	−2.4	—
	[6]Dewar benzene → [6]p.c.	—	3.5	1.5	5.8[g]

[a] ref. [61]

[b] ΔH_f°(benzene) + ΔH_r°(benzene → Dewar benzene) = 19.3 kcal/mol[a] + 60 kcal/mol[c]

[c] ref. [5] for the reaction hexamethylbenzene

[d] estimation based on experimental data [28]

[e] ref. [5] for the reaction hexamethylbenzene, $E_a = 37.2$ kcal/mol ⇒ $\Delta H^{\circ\ddagger} = E_a + RT = 37.8$ kcal/mol at 300 K

[f] ref. [11], $E_a = 20.5$ kcal/mol ⇒ $\Delta H^{\circ\ddagger} = E_a + RT = 21.1$ kcal/mol at 300 K

[g] ref. [11]

values (−68.9 + 37.3 = −31.6 kcal/mol with C.I.). The same comment can be presented for the enthalpies of activation $\Delta H^{\circ\ddagger}$, but the changes are smaller than for the reaction enthalpies. Another tendency, which is clear from the data in Table 3, is the fact that the activation enthalpies $\Delta H^{\circ\ddagger}$ for [*n*]paracyclophanes ($n = 6, 7$) ($\Delta H^{\circ\ddagger} \approx 21.6$ kcal/mol with C.I.) are smaller than the homologous values for benzene ($\Delta H^{\circ\ddagger} \approx 27.9$ kcal/mol with C.I.). Provided that the global shapes of the reaction path near the energy minima are the same for the bridged and for the unbridged compounds [43, 44], a schematic drawing of the potential energy profiles associated with each structure (Fig. 7) leads to an intersection which represents the location of the transition state. This intersection is higher in energy in the case of benzene than in the case of the bridged compounds since the minima related to the [*n*]paracyclophanes are located on the reaction path closer to the Dewar benzene isomer than for benzene.

From previous kinetic experiments [12, 11, 5], it is known that the preexponential factors A of the Arrhenius law for the isomerisations of disubstituted [6]Dewar benzenes to its [6]paracyclophane isomers are in the order of $A \approx 10^{12}\ s^{-1}$. This value allows the entropy of activation at an experimental

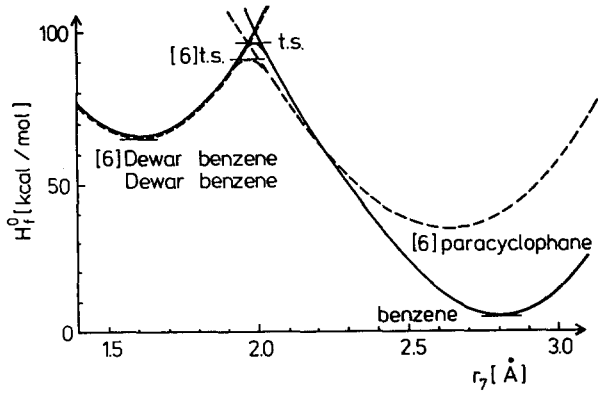

Fig. 7. Schematic representation of the potential energy profiles of the reactions benzene → Dewar benaene (*solid line*) and [6]paracyclophane → [6]Dewar benzene (*dashed line*)

temperature around 330 K [11] to be estimated from the Eyring equation [52] equal to 5.8 cal K^{-1} mol^{-1}. It turns out that our theoretical values (at 300 K) lie in a range which is in an acceptable agreement with this experimental value considering the fact that the experiments have been performed in the liquid phase and not at a constant temperature.

These values show that the semiempirical calculations work well for the thermal valence isomerisations of benzene, [6]- and [7]paracyclophane to their Dewar benzene isomers. This indicates that the deformation shifts the [n]paracyclophanes on the potential energy surface towards the Dewar benzene isomer, but it "leaves" the surface itself almost unchanged.

3.5 Energetic analysis of the reaction path [n]Dewar benzene → [n]prismane

The energies of the stationary points on the potential energy surface of the reaction prismane → Dewar benzene, i.e. the energy minima of prismane P, Dewar benzene D, the hilltop H and the intermediate I (and I′) and the energies of the transition states *C*1 and *C*2 (and *C*1′ and *C*2′), are given in Table 4. From these data, five sets of quantities, characteristic of the reaction, can be deduced. Four of these are displayed in Fig. 5. They are: (i) $\Delta H^\circ_{r,1}$, the enthalpy of the reaction: prismane P → Dewar benzene D, (ii) $\Delta H^\circ_{r,2}$, the enthalpy of the process: prismane P → intermediate I, (iii) $\Delta H_1^{\circ\ddagger}$, the activation enthalpy of the process: intermediate I → prismane P and (iv) $\Delta H_2^{\circ\ddagger}$, the activation enthalpy of the process: intermediate I → Dewar benzene D. The fifth quantity $\Delta H_3^{\circ\ddagger}$ is the activation enthalpy of the reaction: prismane P → Dewar benzene D, which is equal to: $\Delta H_3^{\circ\ddagger} = \Delta H^{\circ\ddagger}(\mathrm{P} \rightarrow \mathrm{D}) = \Delta H^\circ_{r,2} + \max(\Delta H_1^{\circ\ddagger}, \Delta H_2^{\circ\ddagger})$.

The calculated heats of reaction $\Delta H^\circ_{r,1}$ are about −32 kcal/mol for the unbridged compounds (from the RHF- and the UHF-approaches) and −34 kcal/mol for [6]prismane. They are in very good agreement with experimental data, known for substituted compounds, such as for hexamethylprismane [1] and perfluorohexamethylprismane [2]. Both approaches (UHF and RHF-C.I.) indicate the existence of an intermediate, roughly $\Delta H^\circ_{r,2} = 10$ kcal/mol higher in energy than prismane. No experimental data are yet known about this intermediate.

Since the geometry of the alkyl chain is almost the same in [n]prismanes as in their Dewar benzene isomers and the geometries of the prismane- and Dewar

Table 4. Enthalpies (in kcal mol^{-1}) and entropies at 300 K (in cal K^{-1} mol^{-1}) of the valence isomerisation of prismane. Similar values for valence isomerisation of [7]- and [6]prismane to its Dewar benzene isomers

	Compound/reaction	RHF	UHF	C.I.	exp.	C.I. on [6]Dewar benzene
ΔH_f°	Dewar benzene D	89.6	89.2	74.8	"79.3"[a]	61.0
	hilltop H	—	151.9	149.0	—	128.3
	prismane P	121.9	121.9	120.9	—	95.4
	transition state C1 (D→I)	—	134.9	137.2	—	117.0
	intermediate I	—	130.6	133.9	—	111.0
	transition state C2 (I→P)	—	140.8	139.7	—	118.0
$\Delta H_{r,1}^\circ$	P→D	−32.3	−32.7	−46.1[e]	−26.3[b] −31.0[d]	−34.4[f]
$\Delta H_{r,2}^\circ$	P→I	—	8.7	13.0	—	15.5
$\Delta H_1^{\circ\ddagger}$	I→P	—	10.2	5.8	—	7.0
$\Delta H_2^{\circ\ddagger}$	I→D	—	4.3	3.3	—	6.0
$\Delta H_3^{\circ\ddagger}$	P→D[g]	—	18.9	18.8	30.5[b] 42.1[d]	22.5
S°	Dewar benzene D	63.8	64.0	63.9	—	91.3
	hilltop H	—	62.3	62.6	—	91.7
	prismane P	59.4	59.4	59.7	—	91.9
	transition state C1 (D→I)	—	64.9	64.6	—	93.4
	intermediate I	—	65.2	65.1	—	95.7
	transition state C2 (I→P)	—	63.6	64.4	—	91.7
$S_{r,1}^\circ$	P→D	4.4	4.7	4.2	—	−0.6
$S_{r,2}^\circ$	P→I	—	5.9	5.5	—	3.8
$S_1^{\circ\ddagger}$	I→P	—	−1.7	−0.7	—	−2.3
$S_2^{\circ\ddagger}$	I→D	—	−0.3	−0.5	—	−3.9
$S_3^{\circ\ddagger}$	P→D	—	5.6	5.0	5.1[c] 10.9[d]	1.5

[a] deduced from experimental values, see Table 3
[b] ref. [1] for hexamethylprismane
[c] ref. [62]
[d] ref. [2] for perfluorohexamethylprismane
[e] this value is different from those calculated with RHF and UHF because not all the MOs, crossing along the reaction path, could be used in the C.I. level because of limitations in computation time and storage
[f] since the MO correlation diagrams are almost the same for [6]prismane as for prismane, comment[e] may also hold for [6]prismane
[g] $\Delta H_3^{\circ\ddagger} = \Delta H^{\circ\ddagger}(\mathrm{P}\rightarrow\mathrm{D}) = \Delta H_{r,2}^\circ + \max(\Delta H_1^{\circ\ddagger}, \Delta H_2^{\circ\ddagger})$

benzene skeletons (Table 2) are also almost identical for the bridged and unbridged structures, the reaction enthalpy of [6]prismane is nearly identical to that of the unbridged compound.

The absolute entropies S° at 300 K in the gas phase, calculated for these reactions, are also given in Table 4. It is clear that the Dewar benzenes have

higher absolute entropies than the prismane isomers. However, the reaction entropies ΔS_r° remain small (about 2 cal K^{-1} mol^{-1} for prismane → Dewar benzene, 0.5 cal K^{-1} mol^{-1} for [6]prismane → Dewar benzene) as expected for valence isomerisations which are typically in the range of $\Delta S_r^\circ = -5$ to $+3$ cal K^{-1} mol^{-1} [50]. The reaction entropies for the formation of the intermediate from prismane are also about 2 cal K^{-1} mol^{-1}.

The calculated values for the heats of activation $\Delta H^{\circ\ddagger}$ (Table 4) show that the intermediate is separated by low activation barriers from prismane and from Dewar benzene (3.3 and 5.8 kcal/mol respectively with the C.I approach). Since the intermediate I is not yet known experimentally, the only information obtained from experiment is the activation enthalpy $\Delta H_3^{\circ\ddagger}$ of the reactions of substituted prismanes to their Dewar benzene isomers. However, they depend very much on the substituents (30.5 kcal/mol for hexamethylprismane [1], 42.1 kcal/mol for perfluorohexamethylprismane [2]). Our calculations for the unsubstituted compound lead to 18.8 kcal/mol which is in a reasonable interval within the comparable experimental data of hexamethylprismane and perfluorohexamethylprismane (Table 4).

The activation entropies, $\Delta S_3^{\circ\ddagger}$ are small (about 0 cal K^{-1} mol^{-1}). Experimental data cannot be directly compared to the results of our calculations because they are only known for substituted compounds. These experimental values are measured at temperatures higher than 300 K and in liquid phase (not in the gas phase). However, it turns out that our theoretical values (at 300 K) lie in a range which is in an acceptable agreement with these experimental values.

4 Conclusion

In this work, we have determined the geometries of [n]paracyclophanes, their Dewar benzene and prismane isomers (for $n = 6, 7$) and of the unbridged compounds. The geometrical data found are in good agreement with other theoretical [17, 24, 19] and experimental values [25, 54, 55, 56, 47].

In an attempt to gain insight into some features of the potential energy surfaces involved in the reactions Dewar benzene → benzene and [n]Dewar benzene → [n]paracyclophane ($n = 6, 7$), the transition states of the reactions using the "chain" method [57] have been located. For benzene itself, we find that the maximum symmetry C_{2v} is conserved along the reaction path as postulated in previous work [18]. This does not avoid a crossing of molecular orbitals at a distance of the *para* carbon atoms $r_7 \approx 2.1$ Å. The same crossing was obtained from a simple approximation of the reaction path ($r_7 \approx 2.3$ Å [42]) based on the Fukui method [58, 59].

Almost the same transition state geometries are obtained for the valence isomerisations of benzene and the [n]paracyclophanes with $n = 6$ and 7, giving evidence that the topology of the potential energy surfaces is almost the same in the three cases, independent of the deformation of the aromatic ring. This phenomenon has already been postulated from experimental data by Dreeskamp *et al.* on the valence isomerisation of 9-*t*-butylanthracene [8] and is now confirmed theoretically from our calculations on [n]paracyclophanes.

The quantitative analysis in the case of these reactions shows that, even if the reaction enthalpies of the valence isomerisations change significantly (from $\Delta H_r^\circ = -37.2$ kcal/mol for [6]paracyclophane to $\Delta H_r^\circ = -68.9$ kcal/mol for benzene with CI), the activation enthalpies vary much less ($\Delta H^{\circ\ddagger} = 21.7$ kcal/mol

for [6]paracyclophane to $\Delta H_r^\circ = -27.9$ kcal/mol for benzene with CI). These results are in a good agreement with experimental data [12, 11, 5]. The reaction entropies ΔS_r° are found to be in the interval of $\Delta S_r^\circ \approx -3$ to -5 cal K^{-1} mol^{-1}. They are typical for valence isomerisations (see examples in [50]). Moreover, we find the activation entropies for these reactions to lie within $\Delta S^{\circ\ddagger} \approx -2$ to 2 cal K^{-1} mol^{-1} at $T = 300$ K. They are in good agreement with the values calculated from the experimental Arrhenius factors of disubstituted [6]paracyclophanes which we determined in a previous study [12].

The reaction Dewar benzene → benzene passes through a single transition state. The same form of the potential energy surface was postulated for the reaction prismane → Dewar benzene in other work [1]. But from a detailed analysis of the reaction path obtained from our calculations, we find that the conservation of the maximum symmetry C_{2v} leads to a hilltop in the potential energy surface but not to a transition state. Transition states are found in the subgroup C_s. Furthermore, we are able to conclude the existence of an intermediate, i.e. a local minimum on the potential energy surface. This intermediate is a triplet biradical in which one of the two C–C bonds, which are broken in the reaction prismane → Dewar benzene, still exists. For [*n*]prismanes ($n = 6, 7$) no significant qualitative or quantitative change of the reaction due to the alkyl bridge can be found.

These results allow us to suggest a reaction mechanism for the experimentally observed reactions of disubstituted [6]prismanes:

Observation 1. The prismane isomers are fairly stable at room temperature; reaction only occurs at higher temperatures [12]. This follows directly from the calculated activation enthalpies (Table 4) for this symmetry-forbidden reaction [41] which are in good agreement with experimental data.

Observation 2. The thermal reaction leads to the [*n*]paracyclophanes and to ortho-bridged compounds [12]. This follows from the potential energy surfaces of the reactions [6]prismane → [6]Dewar benzene (Fig. 5) and [6]Dewar benzene → [6]paracyclophane (Fig. 7) and from the fact that no direct reaction path from the prismane isomers to benzene or to [6]paracyclophane is found in our studies. Therefore, the first step of the thermal reaction of [6]prismane is the formation of the Dewar benzene isomer via the intermediate. Depending upon which σ-bond of prismane is opened to give the intermediate, the para- or the ortho-bridged Dewar benzene is obtained (Fig. 8). None of these two processes is strongly favoured, since the ortho-bridged biradical is only 4.5 kcal/mol (with the UHF approach) more stable than the para-bridged one, and therefore, the quantites are expected to be almost the same for the two Dewar benzene isomers. Under the reaction conditions of the experiments (temperature about 100°C [12]), they give [6]paracyclophanes (from the para-bridged Dewar benzenes) or ortho-bridged benzenes (from the ortho-bridged Dewar benzenes) in the same quantities. The same results are obtained experimentally, where the thermal reactions of disubstituted [6]prismanes give a maximum of about 40% of the [6]paracyclophane isomer [53]. We are also able to give quantitative data, such as reaction and activation enthalpies and entropies in addition to these qualitative aspects. They are in a satisfying agreement with experimental values known for several substituted prismane derivatives [1, 2].

From these considerations, we can conclude that the semiempirical method MNDO with configuration interaction or with the UHF approximation can be expected to be well adapted to reproduce experimental results for the valence isomerisations benzene → Dewar benzene → prismane and the para-bridged com-

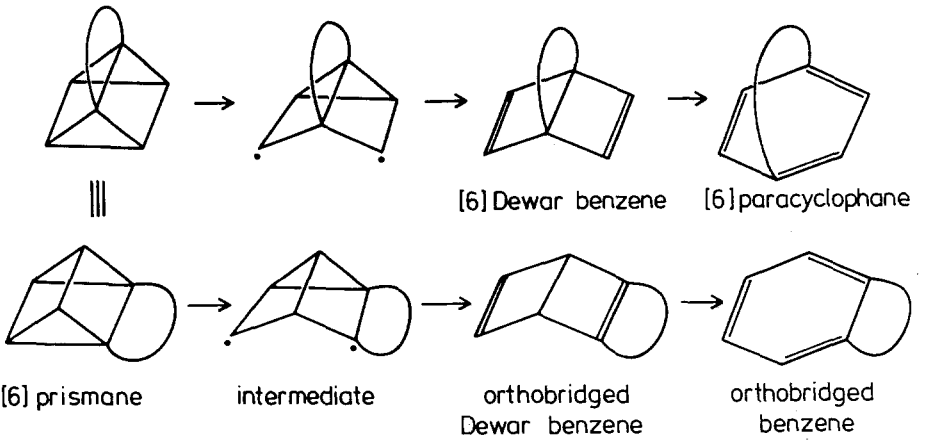

Fig. 8. Reaction mechanism for the thermal ring opening of [6]prismane

pounds. Moreover, they allow information to be obtained that is not yet known experimentally, for example the geometry of an intermediate and the transition states.

Acknowledgements. All computations were performed on the supercomputers IBM 3090J/VF at the "Rechenzentrum der TU Braunschweig" and the "Centre Inter Régional de Calcul Electronique (C.I.R.C.E.)" at Orsay. They are thanked for having provided the time needed for the calculations. Moreover, we gratefully acknowledge the "Deutsche Akademische Austauschdienst (D.A.A.D.)" and the "Fonds der Chemischen Industrie" for the award of a fellowship.

References

1. Adam W, Chang JC (1969) Int J Chem Kinetics I, 487
2. Lemal DM, Dunlap Jr LH (1972) J Am Chem Soc 94:6562
3. Kanada K, Imamura A (1986) J Mol Struct (Theochem) 136:111
4. Wingert H, Regitz M (1986) Chem Ber 119:244
5. Oth JFM (1968) Angew Chem 80:633
6. Bryce-Smith D, Gilbert A (1976) Tetrahedron 132:1309
7. (a) Mandella WL, Franck RW (1973) J Am Chem Soc 95:971
   (b) Franck RW, Mandella WL, Falci KJ (1975) J Org Chem 40:327
8. Jahn B, Dreeskamp H (1984) Ber Bunsenges Phys Chem 88:42
9. Liebe J, Wolff C, Krieger C, Weiss J, Tochtermann W (1985) Chem Ber 118:4144
10. Tobe Y, Ueda KI, Kakiuchi K, Kai Y, Kasai N (1986) Tetrahedron 42(6):1851
11. Dreeskamp H, Kapahnke P, Tochtermann W (1988) Radiat Phys Chem 32(3):537
12. Bockisch F, Dreeskamp H, von Haugwitz T, Tochtermann (1991) W Chem Ber 124:1831
13. Meisl M, Janoschek R (1986) J Chem Soc Chem Commun 1066
14. Palmer MH (1987) J Mol Struct 161:333
15. Latajka Z, Ratajczak H, Orville-Thomas WC, Ratajczak E (1972) J Mol Struct 12:492
16. Latajka Z, Ratajczak H, Orville-Thomas WC, Ratajczak E (1981) J Mol Struct 86:91
17. Newton MD, Schulman JH, Manus MM (1974) J Am Chem Soc 96:17
18. Dewar MJS, Ford GP, Rzepa HS (1977) J Chem Soc Chem Commun 728
19. Bews JR, Glidewell C (1982) J Mol Struct Theochem 86:197
20. Allinger NL, Sprague TJ (1973) J Am Chem Soc 95:3893
21. Allinger NL, Sprague TJ, Liljefors T (1974) J Am Chem Soc 96:5100
22. (a) Bickelhaupt F, de Wolf WH (1988) Recl Trav Chim Pays-Bas 107:459
   (b) Jenneskens LW (1986) Small cyclophanes; Aromaticity under strain. Dissertation, Amsterdam

(c) Kostermans GBM (1989) Synthesis and properties of very small [*n*]cyclophanes. Dissertation, Amsterdam
(d) Kostermans GBM, Bobeldijk M, de Wolf WH, Bickelhaupt F (1987) J Am Chem Soc 109:2471
23. Schmidt H, Schweig A, Thiel W (1978) Chem Ber 111:1958
24. (a) Remington RB, Lee TJ, Schaefer III HF, (1986) Chem Phys Lett 124(3):199
(b) Schaefer III HF, Rice JE, Lee TJ, Remington RB, Allen WD, Allen D (1987) J Am Chem Soc 109:2902
(c) Lee TJ, Rice JE, Remington RB, Schaefer III HF (1988) Chem Phys Lett 150(1,2):63
(d) Lee TJ, Rice JE, Allen WD, Remington RB, Schaefer III HF (1988) Chem Phys 123:1
25. Allinger NL, Walter TJ, Newton MG (1974) J Am Chem Soc 96:4588
26. Dewar MJS, Thiel W (1977) J Am Chem Soc 99:4899
27. Liotard DA, Healy EJ, Ruiz JM, Dewar MJS, AMPAC 2.1, QCPE 506 (version 2.14 is available from the authors)
28. Bockisch F, Rayez JC, Liotard D, Duguay B, J Comp Chem, to be published
29. McWeeny R, Sutcliffe BT (1969) Methods of molecular quantum mechanics. Academic Press, NY
30. (a) for a general description of CI methods see [29]
(b) for the CI algorithm implemented in AMPAC 2.14 see: Armstrong DR, Fortune R, Perkins PG, Stweard JJP (1972) J Chem Soc Faraday Trans 2, 68:1839
31. McIver JW, Stanton RE (1972) J Am Chem Soc 94:8618
32. Ishida K, Morokuma K, Komornicki A (1977) J Chem Phys 66:2153
33. Fukui K (1970) J Phys Chem 74:4161
34. Fukui K, Kato S, Fujimoto H (1975) J Am Chem Soc 97:1
35. Tachibana A, Fukui K (1978) Theor Chim Acta 49:321
36. Basilevsky MV (1977) Chem Phys 24:81
37. Müller H (1980) Angew Chem Int Ed Engl 19:1
38. Komornicki A, McIver JW (1974) J Am Chem Soc 96:5798
39. Murrell JN, Laidler KJ (1975) J Am Chem Soc 97:3632
40. Atkins PW (1990) Physical chemistry, 4th ed. Oxford Univ Press, p 594
41. Woodward RB, Hoffmann R (1970) The conservation of orbital symmetry. Verlag Chemie, Weinheim
42. Tsuda M, Oikawa S, Kimura K (1980) Int J Quant Chem 18:157
43. Hammond GS (1955) J Am Chem Soc 77:334
44. March J (1985) Advanced organic chemistry. Wiley, NY
45. Stanton RE, McIver Jr JW (1975) J Am Chem Soc 97:3632
46. Langseth A, Stoicheff B (1956) Can J Phys 24:350
47. Karl RR, Wang YC, Bauer SH (1975) J Mol Struct 25:17
48. Kassab E, Evleth EM, Dannenberg JJ, Rayez JC (1980) Chem Phys 52:151 and other work cited therein
49. (a) Morse M (1934) Calculus of variation in the large. Amer Math Soc. Colloquium Pub 18
(b) Spanier EG (1966) Algebraic topology. McGraw-Hill, NY
(c) Liotard D (1983) in: Maruani, Serre (eds) Symmetry and properties of non-rigid molecules. Elsevier, NY, p 323
50. Glasstone S, Laidler KJ, Eyring H (1941) The theory of rate processes. McGraw-Hill, NY p 296
51. ibid., (b) p 269
52. ibid., (c) p 295
53. Bockisch F, Dreeskamp H, unpublished work
54. Langseth A, Stoicheff B (1956) Can J Phys 24:350
55. Cardillo MJ, Bauer SH (1970) J Am Chem Soc 92:2399
56. Tobe Y, Udea KI, Kakiuchi K, Odaira Y, Kai Y, Kasai N (1986) Tetrahedron, 42(6):1858
57. Liotard D, Penot JP (1981) in: Dora JD, Demongeot J, Lacolle B (eds) Numerical methods in the study of critical phenomena. Springer-Verlag, Heidelberg Berlin New York
58. Fukui K, Kato S, Fujimoto H (1975) J Am Chem Soc 97:1
59. Ishida K, Morokuma K, Komornicki A (1977) J Chem Phys 66:2153
60. Andersen B, Seip HM, Beagley B (1969) Acta Chem Scand 23:1837
61. Aylward GH, Findlay TJ (1981) Datensammlung Chemie in SI-Einheiten, 2nd ed. Verlag Chemie, Weinheim
62. Oth JFM (1968) Recl Trav Chim Pays-Bas 87:1185